Method of Extending Hyperfine Coherence Times in $Pr^{3+}:Y_2SiO_5$

E. Fraval,* M. J. Sellars, and J. J. Longdell

Laser Physics Center, Research School of Physical Sciences and Engineering, Mills Road, Australian National University, Acton 0200, Australia

(Received 7 July 2003; published 19 February 2004)

In this Letter, we present a method for increasing the coherence time of praseodymium hyperfine ground state transitions in $Pr^{3+}:Y_2SiO_5$ by the application of a specific external magnetic field. The magnitude and angle of the external field is applied such that the Zeeman splitting of a hyperfine transition is at a critical point in three dimensions, making the first order Zeeman shift vanishingly small for the transition. This reduces the influence of the magnetic interactions between the praseodymium ions and the spins in the host lattice on the transition frequency. Using this method a phase memory time of 82 ms was observed, a value 2 orders of magnitude greater than previously reported. It is shown that the residual dephasing is amenable to quantum error correction.

DOI: 10.1103/PhysRevLett.92.077601 PACS numbers: 76.70.Hb, 03.67.Pp, 76.30.Kg, 76.60.–k

There is growing interest in the use of nuclear spin states associated with dopant ions in a solid state host to store and manipulate quantum information [1–3]. These applications require the relevant spin transitions to have long coherence times. This can be challenging to achieve in a solid state system due to magnetic interactions between the dopant ion and spins within the host. A spin-free host can be utilized to minimize these interactions [2]; however, not all dopant species of interest are chemically compatible with such hosts. An example of a class of dopants where no satisfactory spin-free host has been identified is the rare earth ions. Because of the potential to manipulate their spin states optically, the use of rare earth ions has been proposed in a number of quantum information applications [1,3]. In this Letter, we investigate the decoherence in the ground state hyperfine transitions in $Pr^{3+}:Y_2SiO_5$ and demonstrate a new method for increasing their coherence times. This technique is expected to be applicable to a wide range of spin systems.

$Pr^{3+}:Y_2SiO_5$ was chosen to investigate since, along with its use in a quantum computing architecture having been proposed by Ichimura *et al.* [1], it has already been used in slow and stopped light demonstrations [4,5]. While the population lifetime is long ($\sim$100 s [6]) the longest coherence time (T_2) stated in the literature for a ground state hyperfine transition in $Pr^{3+}:Y_2SiO_5$ is 500 μs [7]. This is likely to be insufficient for practical quantum computing applications given that the hyperfine transition frequency is $\sim$10 MHz, limiting the Rabi frequencies of any driving field to less than a few megahertz so as to be transition specific. This allows only of the order of 1000 operations to be completed within T_2.

Yttrium orthosilicate has symmetry given by the C_{2h}^6 space group [8] with 2 f.u. Y_2SiO_5 per translational unit. This creates two crystallographically inequivalent sites at which the Pr can substitute for Y, labeled "site 1" and "site 2" [9]. Each site, in fact, consists of a pair of magnetically inequivalent sites related by the crystal's C_2 axis, labeled "a" and "b." The Pr sites in Y_2SiO_5 have electronic singlet ground states with hyperfine ground state interactions described by the following Hamiltonian:

$$H = \boldsymbol{B}\cdot\boldsymbol{M}\cdot\boldsymbol{I} + \boldsymbol{I}\cdot\boldsymbol{Q}\cdot\boldsymbol{I}, \tag{1}$$

where $\boldsymbol{B}$ is the magnetic field vector, $\boldsymbol{I}$ is the vector of nuclear spin operators, $\boldsymbol{M}$ is the effective Zeeman tensor combining nuclear and electronic Zeeman interactions, and $\boldsymbol{Q}$ is the effective quadrupole tensor combining the quadrupole and second order magnetic hyperfine interaction, known as the pseudoquadrupole [10]. The one naturally occurring isotope of Pr has a nuclear spin of 5/2. $\boldsymbol{M}$ and $\boldsymbol{Q}$ for site 1 were recently determined for $Pr^{3+}:Y_2SiO_5$ to be

$$\begin{aligned}\boldsymbol{Q} &= R(\alpha,\beta,\gamma)\begin{bmatrix}-E & 0 & 0\\ 0 & E & 0\\ 0 & 0 & D\end{bmatrix}R^T(\alpha,\beta,\gamma),\\ \boldsymbol{M} &= R(\alpha,\beta,\gamma)\begin{bmatrix}g_x & 0 & 0\\ 0 & g_y & 0\\ 0 & 0 & g_z\end{bmatrix}R^T(\alpha,\beta,\gamma),\end{aligned} \tag{2}$$

where $E = 0.5624$ MHz and $D = 4.4450$ MHz, $(g_x, g_y, g_z) = (2.86, 3.05, 11.56)$ kHz/G, and the Euler angles are $(\alpha, \beta, \gamma) = (-99.7, 55.7, -40)$ [11]. These values are for the crystal aligned with the C_2 axis in the y direction, and the z axis is the direction of linear polarization of the praseodymium optical transitions. These tensors are highly anisotropic due to the low symmetry of the site.

The dominant dephasing mechanism for the Pr hyperfine ground states in Y_2SiO_5 is due to magnetic interactions with the Y nuclear spins in the host. Yttrium has a nuclear spin of 1/2 and a gyromagnetic ratio of $g_n = 209$ Hz/G. Nearest neighbor Y ions induce a magnetic field at the Pr site of the order of 0.1 G. The direct

magnetic dipole-dipole interaction between the Pr and a nearest neighbor Y ion is of the order of hundreds of hertz. This interaction can induce decoherence via two mechanisms. The first mechanism is that the Y ions can exchange spin with each other, resulting in a fluctuating magnetic field at the Pr site. For resonant Y nuclei the rate of exchange between two nearest neighbor ions is of the order of tens of hertz. The second mechanism involves the excitation of nearly degenerate transitions where one or more Y spin flips are induced along with the desired change in the Pr hyperfine state.

To suppress these dephasing mechanisms for a given Pr ground state hyperfine transition, we propose applying a specific magnetic field magnitude and direction such that the transition's linear Zeeman shift about this field value is zero. Necessary conditions for this technique to be applicable are zero field spin state splittings and the ability to apply a magnetic field such that the Zeeman splitting is comparable to the zero field splittings. While we have chosen to demonstrate this technique using a site of C_1 symmetry, critical points can also be found using a Hamiltonian for a system with axial symmetry. The technique is not applicable to sites with higher symmetry, as these do not have zero field spin state splittings.

Using Eq. (2) and the parameters for site 1 given above, all the magnetic field values resulting in a zero first Zeeman shift were identified. The case chosen to experimentally investigate was at a magnetic field of $\boldsymbol{B}_{\mathrm{CP}} = \{732, 173, -219\}$ G on the $m_I = +1/2 \leftrightarrow +3/2$ transition at 8.63 MHz as it was found to have the smallest second order Zeeman shift. Around this magnetic field value the transition energy as a function of magnetic field has a turning point in the y and z axes, while the x axis has a slow inflection point. As the required magnetic field was not along the crystal's C_2 axis the degeneracy between site 1a and site 1b was lifted with only the site 1a ions being at the critical point.

Raman heterodyne two and three pulse spin echoes were used to investigate the decoherence and spectral diffusion in the ground state hyperfine transitions [7] (Fig. 1). The experiment was performed using a Coherent 699 frequency stabilized (1 MHz FWHM) tunable dye laser tuned to the ${}^3H_4 - {}^1D_2$ transition at 605.977 nm. The laser power incident on the crystal was 40 mW, focused to ~ 100 μm, and was gated using a 100 MHz acousto-optic modulator such that there was no laser radiation applied to the sample during the rf pulse sequence (Fig. 1). The Raman heterodyne signal is detected by a photodiode with 250 MHz bandwidth with the intensity of the signal measured by a spectrum analyzer locked to the hyperfine frequency of interest. The rf Rabi frequency of the applied pulses was $\Omega_{\mathrm{rf}} = 300$ kHz. The Pr^{3+}:Y_2SiO_5 (0.05% concentration) crystal was held at ~ 1.5 K for the duration of the experiment. The laser prepared a population difference in the excited ions for 5 s before the pulse sequence and was scanned over 1.2 GHz of the optical transition to avoid hole burning effects. The laser is off during the rf pulse sequence to minimize coherence loss from optical pumping.

The magnetic fields were supplied by two superconducting magnets: one along the z axis, the other in the horizontal plane. The sample was then rotated by $(13 \pm 0.5)°$ to provide the correct ratio of fields along the x and y axes for the critical point in magnetic field space. Coarse adjustment of the field was done by comparing the Raman heterodyne spectrum to theoretical simulations as shown in Fig. 2. Fine adjustment of the magnetic field utilized perturbing coils along each axis and associated lock-in amplifiers to perform field sensitivity measurements on the frequency of the $m_I = +1/2 \leftrightarrow +3/2$ transition. The rotation of the sample and the current

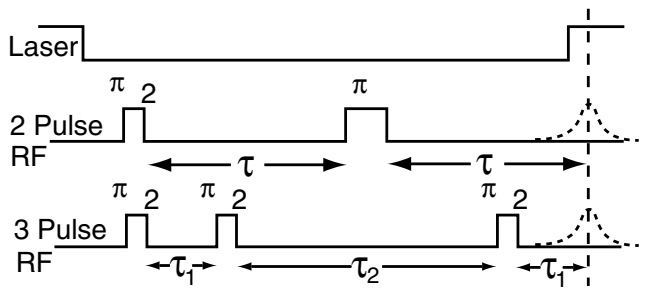

FIG. 1. Two and three pulse echo sequences. π pulse duration was 40 μs and the laser was turned off 150 μs before the pulse sequence and turned on 100 μs before the echo.

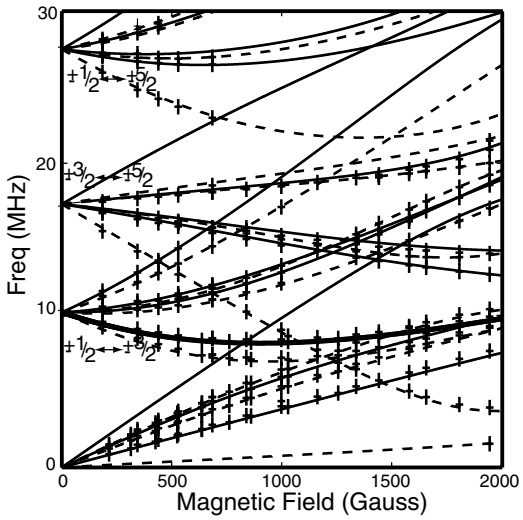

FIG. 2. Spectrum of hyperfine transitions showing experimentally measured points as the magnetic field is applied in the x direction, confirming the Hamiltonian used to model the system. Site 1a transitions are solid lines while site 1b are dashed lines. The transition used to investigate the critical point is bold. While the critical point investigated is not shown here, since it requires fields in the y and z directions, the behavior of the system exploited by the concept is clearly visible.

driving the magnets were iteratively adjusted to minimize the sensitivity of the desired transition. Final adjustments of the field values were made by minimizing the echo decay rate. The magnetic field values were accurate to within ± 0.1 G of the critical point.

The two pulse echo data (Fig. 3) show three echo sequences at the critical point magnetic field configuration with the zero field echo sequence for reference. Since the field configuration is transition specific, the $m_I = +1/2 \leftrightarrow +3/2$ transition at site 1a is at a critical point while the two other transitions are not.

At low magnetic field (0.5 G) directed along the x axis, T_2 of the $m_I = +1/2 \leftrightarrow +3/2$ transition was measured as 550 μs, in agreement with previous measurements [7].

With the application of the critical point magnetic field all the transitions studied showed a significant increase in the coherence time. For the $m_I = +3/2 \leftrightarrow -3/2$ transition T_2 was 5.86 ms while for the $m_I = +1/2 \leftrightarrow +3/2$ transition at site 1b it was 9.98 ms (Fig. 3). Applying a field lifts the degeneracy of the Y spin states and inhibits Pr transition involving single Y spin flips, as observed in analogous systems [12]. This can be understood by considering the Y quantization axis. At zero field the Y quantization axis is locally defined by the Pr ion. Therefore, a change in the spin state changes the quantization axis, mixing the Y spin states and resulting in a high spin flip probability. When the applied field exceeds the field due to the Pr at the Y site, the Pr induced Y spin flip transition probability decreases linearly with an increase in the applied magnetic field. Pr induced Y spin flips were undetectable with an applied field of 30 G in any direction and the coherence time did not significantly change over the range of 30 G to 1 kG. Therefore, we conclude that other dephasing mechanisms dominate with applied fields greater than 30 G.

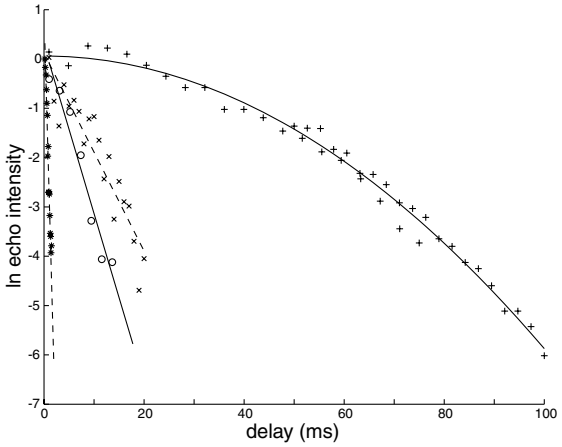

FIG. 3. Two pulse echo sequences taken at the critical point magnetic field $\boldsymbol{B}_{\mathrm{CP}} = \{732, 173, -219\}$ G for transition $m_I = +1/2 \leftrightarrow +3/2$ at site 1a (+). The $m_I = +1/2 \leftrightarrow +3/2$ site 1b transition (×); the $m_I = -3/2 \leftrightarrow +3/2$ transition (○) and the low field (0.5 G) $T_2 = 500$ μs decay line shown for comparison.

The echo decay for the $m_I = +1/2 \leftrightarrow +3/2$ at site 1a is significantly slower than for the other two transitions and is clearly not described by a simple exponential. A T_2 simple exponential decay is characteristic of a magnetic dipole-dipole dephasing interaction with a concentrated spin system reconfiguring much faster than the time scale of the echo sequence [13]. Exponential decay with a quadratic time dependence [Eq. (3)] is characteristic of a spectral diffusion process due to magnetic dipole-dipole interactions with a spin system that reconfigures much slower than the time scale of the echo sequence as shown by Mims [14]. This coherence decay is described by a Lorentz kernel with a width increasing linearly with time at a rate of 47.3 Hz/s [14]. The phase memory T_M is used to characterize the decoherence rate of the system. In the present case the T_M was determined to be 82 ms.

$$I(2t) = I_0 \exp\left[-\left(\frac{2t}{T_M}\right)^2 \right]. \tag{3}$$

To investigate the diffusion process over longer time scales, a series of three pulse echo measurements were made. Within each of the series shown in Fig. 4 the delay between the first two pulses (τ_1) is held constant while the delay between the second and third pulses (τ_2) is varied.

A comparison is made with the same transitions as used in the two pulse echo study. Comparing echo

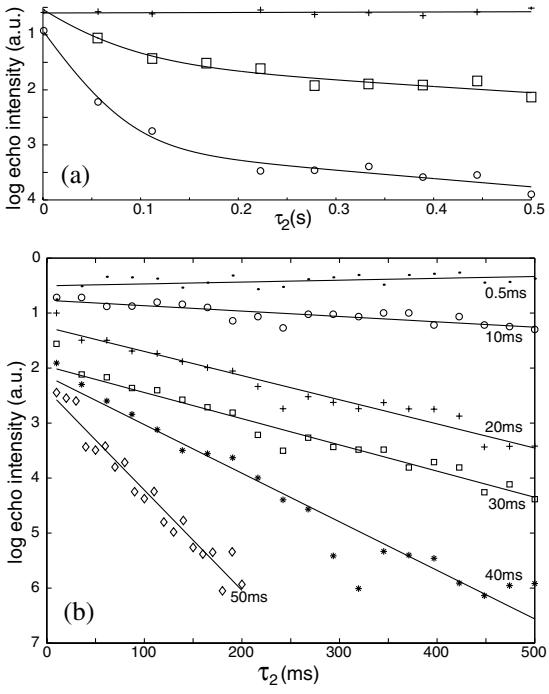

FIG. 4. Three pulse echo sequences taken at (a) $m_I = +1/2 \leftrightarrow +3/2$ transition at site 1a (+) and site 1b (□), $m_I = -3/2 \leftrightarrow +3/2$ transition (○); both traces were taken with $\tau_1 = 2.5$ ms. The delay τ_2 is measured on the x axis, (b) critical point on transition $m_I = +1/2 \leftrightarrow +3/2$ at site 1a. The τ_1 delay for each echo sequence is labeled on the fit line.

sequences with the same τ_1 on the different transitions shows a clear difference between the critical point and the other two transitions [Fig. 4(a)]. The $m_I = -3/2 \leftrightarrow +3/2$ and the site 1b $m_I = +1/2 \leftrightarrow +3/2$ transitions have a clearly biexponential decay: a fast initial decay, reducing to a slow decay for $\tau_2 > 200$ ms. With a τ_1 of 2.5 ms no spectral diffusion was observed on the critical point transition.

The biexponential decay is attributed to the existence of a "frozen core" [15,16]. A frozen core is formed by the Pr ion detuning nearby Y ions from the bulk Y, thereby inhibiting mutual Y spin flips within the frozen core. A strong frozen core is expected due to the Pr magnetic moment being over an order of magnitude larger than that of Y, and the complexity of the Y_2SiO_5 unit cell places each Y ion a unique distance from the Pr ion and therefore has a unique detuning. Although a frozen core has not been reported in Pr^{3+}:Y_2SiO_5, it has been observed in directly analogous systems [16]. On short time scales the rapid spin flips of the bulk Y ions dominate the dephasing. Since the bulk Y are well removed from the Pr ion, they only weakly perturb the transition frequency. On longer time scales the frozen core Y spin flips dominate the dephasing as they induce larger but less frequent frequency shifts. Given that the slow spectral diffusion has not plateaued for the longest τ_2 used, the correlation time of the frozen core is comparable to or longer than 0.5 s.

Further investigation of the three pulse echoes on the critical point transition (Fig. 4) shows that for all values of τ_1 only a single, slow exponential decay was observed. Therefore, dephasing of the critical point transition is dominated at all time scales by the frozen core Y spin flips. The fact that the bulk Y dephasing contribution is absent for the site 1a $m_I = +1/2 \leftrightarrow +3/2$ transition and present for the other two transitions is consistent with the dephasing at the critical point being due to second order Zeeman interactions. Further, it also explains the $\exp(t^2)$ time dependence of the two pulse echo decay since the dephasing process is slow compared to the echo time scale, resulting in a dephasing behavior [14]. This suggests that the applied field is accurate to the order of a Pr-Y interaction strength from the ideal critical point. Further optimization of the applied field is therefore unlikely to produce a significant gain in coherence time.

Using the method described above, a regime has reached where the correlation time of the dephasing interaction is extremely long compared to the duration of readily achievable rf pulses. This is exactly the regime required for effective implementation of NMR phase cycling schemes such as the Carr-Purcell-Mieboom-Gill (CPMG) pulse sequence, which has recently been reinterpreted as a quantum error correction scheme [17–19]. The CPMG pulse sequence consists of a pair of hard rephasing pulses (π) separated by the cycling time. This technique is effective at minimizing dephasing if the pulse sequence can be applied faster than the reconfiguration time of the dephasing mechanism. With our current experimental equipment, a transition specific hard rf π pulse can be applied in 1 μs while the echo decay is characteristic of a dephasing process with a correlation time much slower than T_M (82 ms). Therefore, this technique is expected to be effective at increasing the coherence time of the system.

We have shown that a phase memory time of 82 ms can be achieved for Pr^{3+}:Y_2SiO_5 by using an external magnetic field to minimize the transition sensitivity to magnetic field fluctuations. Directions to further reduce the residual dephasing mechanism have been identified. We have shown that even in hosts containing nuclear spins it is possible to obtain spin based qbits that have coherence properties suitable for sophisticated quantum computing demonstrations.

*Electronic address: elliot.fraval@anu.edu.au

[1] K. Ichimura, Opt. Commun. **196**, 119 (2001).
[2] B. Kane, Nature (London) **393**, 133 (1998).
[3] N. Ohlsson, R. K. Mohan, and S. Kröll, Opt. Commun. **201**, 71 (2002).
[4] A. V. Turukin, V. S. Sudarshanam, M. S. Shahrier, J. A. Musser, B. S. Ham, and P. R. Hemmer, Phys. Rev. Lett. **88**, 023602 (2002).
[5] K. Yamamoto, K. Ichimura, and N. Gemma, Phys. Rev. A **58**, 2460 (1998).
[6] N. Ohlsson, M. Nilsson, and S. Kröll, quant-ph/0301157.
[7] B. S. Ham, M. S. Shahriar, and P. R. Hemmer, Phys. Rev. B **58**, R11825 (1998).
[8] M. J. Buerger, *International Tables For X-Ray Crystallography* (Kynoch Press, Birmingham, England, 1969), 3rd ed.
[9] R. W. Equall, R. L. Cone, and R. M. Macfarlane, Phys. Rev. B **52**, 3963 (1995).
[10] J. M. Baker and B. Bleaney, Proc. R. Soc. London, Ser. A **245**, 156 (1958).
[11] J. J. Longdell, M. J. Sellars, and N. B. Manson, Phys. Rev. B **66**, 035101 (2002).
[12] N. Manson, M. J. Sellars, P. T. H. Fisk, and R. S. Meltzer, J. Lumin. **64**, 19 (1995).
[13] B. Herzog and E. L. Hahn, Phys. Rev. **103**, 148 (1956).
[14] W. B. Mims, Phys. Rev. **168**, 370 (1968).
[15] A. Szabo, Opt. Lett. **8**, 486 (1983).
[16] L. L. Wald, E. L. Hahn, and M. Lunac, J. Opt. Soc. Am. B **9**, 789 (1992).
[17] L. Viola and S. Lloyd, Phys. Rev. A **58**, 2733 (1998).
[18] D. Vitali and P. Tombesi, Phys. Rev. A **59**, 4178 (1999).
[19] M. S. Byrd and D. A. Lidar, Phys. Rev. Lett. **89**, 047901 (2002).